

pubs.acs.org/est Article

# Biocrude Oil from Algal Bloom Microalgae: A Novel Integration of Biological and Thermochemical Techniques

Jamison Watson, Megan Swoboda, Aersi Aierzhati, Tengfei Wang, Buchun Si,\* and Yuanhui Zhang\*



**Cite This:** *Environ. Sci. Technol.* 2021, 55, 1973–1983



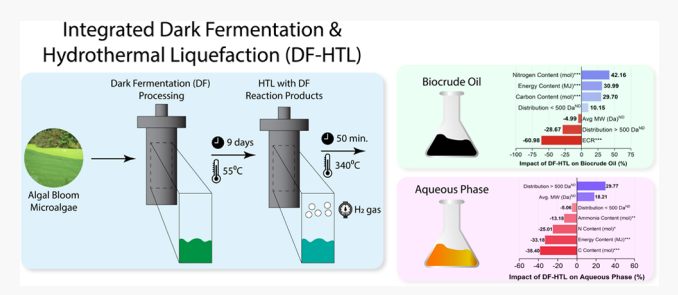
**ACCESS** 

III Metrics & More

Article Recommendations

**Supporting Information** 

ABSTRACT: Algal bloom microalgae are abundant in polluted water systems, but their biocrude oil production potential via hydrothermal liquefaction (HTL) is limited. This study proposed a novel process that combined biological (dark fermentation) and thermochemical (HTL) techniques aimed at changing the feedstock characteristics to be more suitable for thermochemical conversion, herein named integrated dark fermentation—hydrothermal liquefaction (DF-HTL). DF-HTL conversion of algae significantly enhanced the biocrude oil yield (wt %), carbon content (mol), energy content (MJ), and energy conversion ratios



by 9.8, 29.7, 40.0, and 61.0%, respectively, in comparison to the control. Furthermore, DF-HTL processing significantly decreased the aqueous byproduct yield (wt %), carbon content (mol), nitrogen content (mol), and ammonia content (mol) by 19.0, 38.4, 25.0, and 13.2%, respectively, in comparison to the control. Therefore, DF-HTL reduced the environmental impact associated with disposing of the wastewater byproduct. However, DF-HTL also augmented the nitrogen content (mol) of the biocrude oil by 42.2% in comparison to the control. The benefits of DF-HTL were attributed to the increased acid content, the incorporation of  $H_2$  as a processing gas, and the enhancement of the Maillard reaction, which shifted the distribution of reaction products from the aqueous phase to the biocrude oil phase. This article provides insights into the efficacy of a novel integrated biological—thermochemical processing method with distinct environmental and energetic advantages over conventional HTL that heightens the biocrude oil yield for feedstocks with a high carbohydrate and a high protein content.

#### 1. INTRODUCTION

Nutrient pollution of lakes and rivers is becoming a dire concern for countries around the world. In the United States, the Environmental Protection Agency has estimated that over 3 500 000 acres of lakes and reservoirs are impaired by the accumulation of nitrogen and phosphorus. 2,3 A byproduct of nutrient pollution is the accumulation of harmful algal blooms. Previous studies noted that algal blooms can produce toxins harmful to humans, cause eutrophication to bodies of water, and disrupt the ecological balance.<sup>4,5</sup> However, the United States is not the only country uniquely facing this problem. A previous study demonstrated that accelerated eutrophication directly impacted 41% of the lakes in South America, 53% of the lakes in Europe, and 54% of the lakes in the Asia-Pacific region.6 Thus, finding a way to curtail the growth of algal blooms is an essential international problem that needs to be addressed.

In recent years, the Bioenergy Technologies Office of the Department of Energy has classified algal hydrothermal liquefaction (HTL) as a high-impact research area due to its low-cost and environmentally sustainable biomass cultivation and harvesting approach. HTL can be defined as the direct conversion of a high-moisture-content feedstock (70–90 wt %) into biocrude oil by subjecting the feedstock to elevated temperatures (200–380 °C) and pressures (5–28 MPa) in an

oxygen-free environment.<sup>9</sup> However, the HTL process is not conducive to the conversion of high-carbohydrate and high-protein algae feedstocks due to depressed yields along with the production of an oil with poor physical properties.<sup>10</sup> Previous studies have confirmed that lipids are most readily converted to biocrude oil in comparison to proteins and carbohydrates.<sup>11</sup> However, in nature, algae with a high carbohydrate and protein content are omnipresent, whereas the availability of high-lipid-content algae is limited.

Previous studies mostly focused on optimizing HTL operational parameters to augment the biocrude oil quantity. Tian et al. demonstrated that the yield of biocrude oil increased from 11.3 to 18.4% as the holding temperature was increased from 210 to 290 °C and the retention time was increased from 30 to 60 min for the HTL conversion of a high-carbohydrate algae feedstock. <sup>12,13</sup> Li et al. demonstrated that optimizing the reaction temperature and retention time

Received: September 4, 2020
Revised: December 30, 2020
Accepted: December 31, 2020
Published: January 12, 2021





increased the biocrude oil yield of high-protein microalgae, Nannochloropsis sp., by 19.2%. 14 However, additional strategies should be taken to break through the limitation of feedstock composition and sidestep the rapid and violent reactions associated with hydrothermal reactions at elevated temperatures. 15 To that end, we propose a novel process that combines biological (dark fermentation (DF)) and thermochemical (HTL) approaches aimed at changing the feedstock characteristics to be more suitable for thermochemical conversion, herein referred to as integrated dark fermentation (DF) and hydrothermal liquefaction (DF-HTL). We assumed that several potential advantages could be achieved via integration of these two processes: (1) DF could convert carbohydrates into volatile fatty acids while concomitantly producing hydrogen.<sup>16</sup> The resulting products derived from carbohydrates are assumed to be less recalcitrant to subsequent thermochemical degradation, and the produced hydrogen could be incorporated as a processing gas during HTL conversion. (2) Proteins and lipids in algae, which are the main contributors to biocrude oil production via HTL, are recalcitrant to biological degradation via DF. 17-21 Most of these compounds would not undergo biological conversion and could therefore take part in HTL reactions. (3) Biomass particles can be converted into water-soluble compounds after biological conversion. This would accelerate the interactions between carbohydrates and proteins in solution, namely, through the Maillard reaction, which could enhance the oil yield and reduce the yield of aqueous products.

Herein, algal bloom microalgae, which were harvested from Lake Tainter, Wisconsin, were investigated for the novel DF-HTL process. This study aims to achieve the following goals: (1) integrate biological (DF) and thermochemical (HTL) techniques that demonstrate distinct advantages over conventional HTL; (2) understand the benefits and pitfalls of DF-HTL on the resulting biocrude oil and aqueous phase products; (3) reveal the reaction pathway and chemistry behind DF-HTL using model carbohydrate and protein compounds.

## 2. MATERIALS AND METHODS

**2.1. Feedstock and Sludge.** The algal bloom microalgae were harvested from Lake Tainter (44.955N, -91.88W) near Menomonie, Wisconsin from a wind-flocculated bloom. The microalgae were collected by passing the algae through a series of screens to filter out residual debris (Figure S1). Subsequently, 100 and 200- $\mu$ m polypropylene bags were utilized to collect the pure algae samples. The bulk filtrate algae bloom was then stored in a freezer (-24 °C) prior to use. The proximate, ultimate, and metal analysis of the algae along with Lake Tainter water quality data are presented in the Supporting Information (Tables S1–S3).

The inoculum for DF was obtained from an anaerobic digester at the Urbana and Champaign Sanitary District (Urbana, IL). The inoculum was washed using DI water and centrifuged (3000 rpm, 10 min). Then, the inoculum was heat treated (105 °C, 2 h) to enhance the content of hydrogen-producing bacteria. The inoculum had a total solid content of 2.7  $\pm$  0.1% and a volatile matter content of 64.2  $\pm$  0.1%. The contribution of the inoculum sludge on the HTL outputs was considered negligible since the weight ratio was less than 4%

For the model compound experiments, technical grade casein from bovine milk (Sigma-Aldrich, CAS: 9000-71-9) was

utilized as the model protein compound. Highly purified Sigmacell cellulose (Sigma-Aldrich, CAS: 9004-34-6) was utilized as the model carbohydrate polymer. D-Glucose (Sigma-Aldrich, CAS: 50-99-7) was utilized as the model sugar monomer. Acetic acid (Fisher Scientific, CAS: 64-19-7, purity: 99.5%) was utilized as the model sugar produced via fermentation of the model glucose monomer.

**2.2. Dark Fermentation.** DF was conducted in batch mode using 160 mL serum bottles in triplicate. DF experiments were performed at low (25 °C), medium (37 °C), and high (55 °C) temperatures using a water bath. The low, medium, and high DF temperature conditions were labeled DF-L, DF-M, and DF-H, respectively. At the beginning of fermentation, 5 mL of the sludge and 4 g of algae were added into the bottles. DF was conducted using solid-state conditions, namely, dry fermentation (with a total solid content of 20%). Nitrogen gas was then used to purge the bottles of the remaining oxygen to ensure an anaerobic headspace. The control group was prepared in the same manner as the DF conditions; however, the mixture of algae and sludge was stored in a fridge (4 °C) as opposed to a water bath.

2.3. Hydrothermal Liquefaction. HTL model compound experiments and the control experiment were conducted according to the methods described in previous studies.<sup>23,24</sup> In brief, HTL experiments were conducted in a 30 mL stainless steel reactor (Swagelok; Solon, OH). The feedstock mixture was diluted to the desired solid content and then the reactor was sealed. For the model compound binary experiments, the carbohydrate and protein model compounds were added at a 1:1 ratio. Once the feedstock was added, the reactor was purged with N2 three times to ensure the evacuation of all oxygen from the headspace, and then the initial pressure was set to 0.7 MPa. Once the reactor was sealed, the furnace (Thermo Scientific Lindberg Blue M) was set to the designated reaction temperature, and once the temperature was achieved, the reactor was placed in the furnace for the duration of the retention time. Once the reaction was complete, the reactor was cooled and then the gas product was collected using gas bags. Analytical grade dichloromethane (Sigma-Aldrich, CAS: 75-09-2, purity: ≥99.8%) was then added to the reactor to isolate the reaction products. The biocrude oil, gas, and solid residue product yields were calculated by dividing the total dry mass of the reactant by the weight of the product. The yield of the aqueous phase was calculated by the difference between the other three reaction

In contrast to the model compound experiments and the control experiment, the separated DF and HTL of algae as well as the integrated DF-HTL experiments were conducted using a different methodology. Separated DF and HTL experiments of algae were conducted by first subjecting the algae feedstock to DF conditions in a serum bottle at a temperature of 55 °C using a water bath (see Section 2.2). Subsequently, the residue was removed from the serum bottle and placed in the HTL reactor. Finally, HTL reactions were conducted using this fermented feedstock, as previously described above. As for the integrated DF-HTL processing, the HTL reactor was used in place of the serum bottle to conduct DF (in contrast to the separated DF and HTL processes). Once the DF retention time was reached, HTL reactions were conducted immediately without discharging the produced gas. A representative illustration comparing separated DF and HTL of algae and

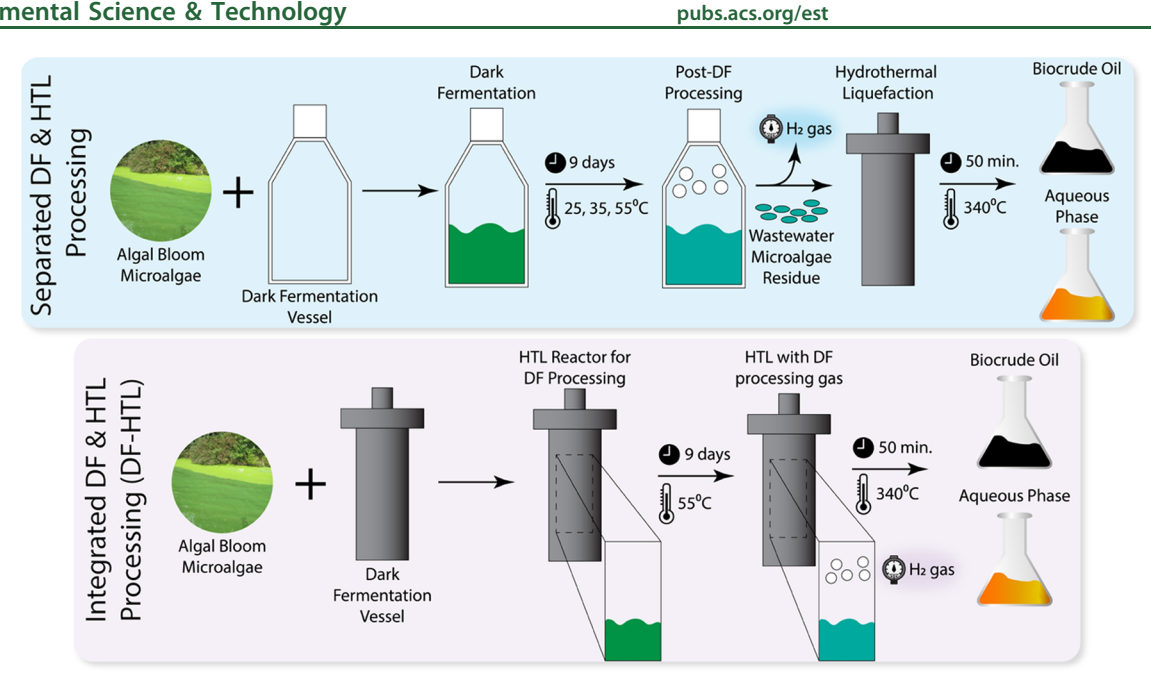


Figure 1. Reaction setup for the separated dark fermentation (DF) and hydrothermal liquefaction (HTL) of algae (DF-L, DF-M, and DF-H) and integrated DF-HTL thermochemical processing experiments.

integrated DF-HTL conversion is presented in Figure 1. All experiments were conducted in duplicate or triplicate. If values deviated by more than 5%, a triplicate experiment was conducted. The reaction setup for the control, separated DF and HTL, DF-HTL, and model compound experiments is presented in the Supporting Information (Table S4).

2.4. Analysis of Products. The gas product after DF was analyzed utilizing a gas chromatograph (Shimadzu gas chromatograph, GC-17A) with a thermal conductivity detector (TCD) packed with silica gel. The column was 18 ft in length and had an outer diameter of 1/8 in. Analysis was conducted by setting the injector, detector, and column temperature to 160, 150, and 140 °C, respectively.

Elemental analysis of the oil and solid product was conducted utilizing a CE440 elemental analyzer (Exeter Analytical; North Chelmsford, MA). The oxygen content was calculated by the difference. The higher heating value (HHV) of the biocrude oil samples was calculated based on Dulong's formula.<sup>25</sup> The total ammonia content of the aqueous phase was measured by diluting aqueous samples (100×) and then using the total nitrogen by the Persulfate Digestion Test 'N Tube method (Hach method 10071). The total ammonia content was tested then utilizing a Nitrogen-Ammonia Nessler reagent set (Hach 2458200). A DR3900 laboratory spectrophotometer (Hach Company; Loveland, CO) was utilized to detect the absorbance for all total nitrogen and total ammonia content tests.

The chemical characterization of the aqueous and biocrude oil samples was conducted via gas chromatography-mass spectrometry (GC-MS) (Agilent Technologies; Santa Clara, CA). All GC-MS data were normalized by the internal standards: 0.1 µM 3-methyl butanoic acid for the aqueous phase and 0.5  $\mu$ M pentadecanoic acid for the biocrude oil. The detailed analytical procedures for GC-MS were previously described in the literature.<sup>26</sup>

High-resolution liquid chromatography-mass spectrometry (LC-MS) was utilized to characterize the aqueous phase samples for the control and the DF-HTL conditions. Samples

were analyzed using the Q-Exactive MS system (Thermo Fisher Scientific; Bremen, Germany) in the Metabolomics Laboratory of the Roy J. Carver Biotechnology Center, University of Illinois at Urbana-Champaign. The LC separation was performed on a Phenomenex Kinetex C<sub>18</sub> column (4.6  $\times$  100 mm<sup>2</sup>, 2.6  $\mu$ m) with mobile phase A (H<sub>2</sub>O with 0.1% formic acid) and mobile phase B (acetonitrile with 0.1% formic acid). The flow rate was 0.25 mL/min. The linear gradient was as follows: 0-3 min, 100% A; 20-30 min, 0% A; and 30.5-36 min, 100% A. The resolution of the full scan mass spectrum was set at 70 000 with a scan range of m/z70-1050, and the automatic gain control (AGC) target was 1  $\times$  10<sup>6</sup> with a maximum injection time of 200 ms.

The mass distributions in the biocrude oil and aqueous phase were analyzed via matrix-assisted laser desporption/ ionization time-of-flight mass spectrometry (MALDI-TOF-MS). MALDI-TOF mass spectra measurements were conducted using a Bruker Autoflex Speed LRF instrument (Bruker Scientific Instruments; Germany) with dual microchannel plate detectors for both linear and reflectron modes. MALDI-TOF was used with Flexcontrol software 3.0 (Bruker Daltonics) for the automatic acquisition of mass spectra in the reflectron positive mode within the range 150-1500 Da. The acceleration voltage was +19 kV. trans-2-[3-(4-tert-Butylphenyl)-2-methyl-2-propenylidene]malononitrile (DCTB) was used as the matrix reagent. Samples used for MALDI-TOF-MS analysis involved the addition of 1  $\mu$ L of the liquid product and 10  $\mu$ L of the matrix solution, then 1  $\mu$ L of this mixture (10 mg/mL) was placed on the MALDI target plate for subsequent testing before being mixed with the matrix.

# 3. RESULTS AND DISCUSSION

3.1. HTL of Algal Bloom Microalgae. A parameter optimization screening was conducted to optimize biocrude oil production for subsequent integration of biological (DF) and thermochemical (HTL) systems. According to the data presented in Figure 2A, the biocrude oil yield first increased and then decreased after reaching a maximum value (41.8%) at

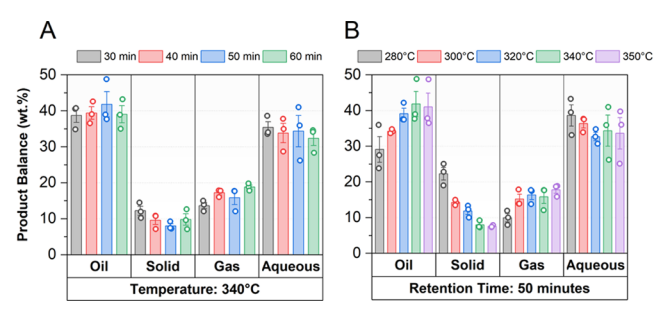


**Figure 2.** Investigation of reaction parameters to optimize biocrude oil production derived from algae. Variations of the biocrude oil yield at a constant temperature (A). Variations of the biocrude oil yield at a constant retention time (B). The open shapes on the column bar represent the values of the individual trials. The column bar represents the average value of the individual trials.

a retention time of 50 min. A similar trend is shown in Figure 2B, in which the biocrude oil yield increased from 29.1% at 280  $^{\circ}$ C to 41.8% at 340  $^{\circ}$ C and then decreased thereafter. Thus, a temperature of 340  $^{\circ}$ C and a retention time of 50 min were selected for subsequent separated DF and HTL of algae experiments.

3.2. Effect of Dark Fermentation on the Hydrothermal Liquefaction of Algal Bloom Microalgae. 3.2.1. Dark Fermentation of Algal Bloom Microalgae. DF-H (55 °C) demonstrated the highest production of H<sub>2</sub>, amounting to a volume of 43.5 mL/g TS. DF-M and DF-L exhibited diminished H<sub>2</sub> production in relation to DF-H, leading to maximum H<sub>2</sub> volumes of 11.1 and 6.0 mL/g TS, respectively (Figure 3A). The large amount of H<sub>2</sub> produced for

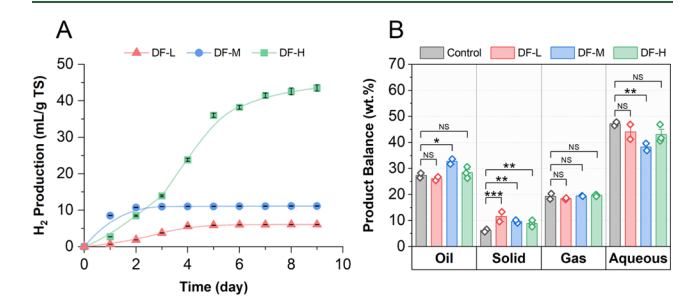


**Figure 3.** Production of hydrogen gas from the DF of algae at 25 °C (DF-L), 35 °C (DF-M), and 55 °C (DF-H) (A). The product balance for the control and the separated DF and HTL (DF-L, DF-M, and DF-H) processing trials conducted at a temperature of 340 °C and a retention time of 50 min (B). \*Denotes p-value <0.10, \*\*denotes p-value <0.05, \*\*\*denotes p-value <0.01, and NS denotes a lack of statistical significance between the treatment and control (p > 0.1). The open shapes on the column bar represent the values of the individual trials. The column bar represents the average value of the individual trials.

the DF-H trial could have been attributed to the thermophilic nature of the inoculum and the increased presence of acidogenic microorganisms at an elevated temperature, thereby favoring acidogenesis/acetogenesis in lieu of methanogenesis. The low production of  $H_2$  in the DF-M and DF-L conditions could have been attributed to the low incubation temperature (25–35 °C). It can be hypothesized that lower temperatures led to the inability of overcoming the energy barrier needed to break the cross-linkage networks of the algal cell wall. This led to a diminished access to glucose since

milder conditions were unable to cleave  $\beta$ -1,4-glycosidic linkages and subsequently produce  $H_2$ .

3.2.2. Separated Dark Fermentation and Hydrothermal Liquefaction Processing of Algal Bloom Microalgae. Product gravimetric results demonstrated that first fermenting algae and using the residue to conduct HTL promoted the production of biocrude oil (Figure 3B). However, this conclusion was only valid for trials DF-M and DF-H, which exhibited increases in the biocrude oil yield by 1.1 and 5.4% compared to the control, respectively. The chemical characteristics of the biocrude oil and the aqueous phase derived from the separated DF and HTL experiments are presented in the Supporting Information (Figures S2–S5).

Increases in the oil yield could have been attributed to multiple factors. One reason could be the elimination of cross-linked carbohydrate materials via DF. The cleavage of carbohydrate cross-linkages between cellulose,  $\beta$ -mannans, and  $\beta$ -galactofuranan during DF may have enhanced the hydrothermal degradability of the resulting intermediate residue, thereby reducing the activation barrier needed to achieve biocrude oil production. Previous studies have demonstrated that cross-linked materials have been shown to resist hydrothermal degradation.

Another explanation could be that DF-M and DF-H conditions were able to better solubilize the protein and carbohydrate substrates, thereby promoting glucose—protein interactions. A previous study noted that synergy exists between the model glucose and protein compounds, which could increase the biocrude oil yield. In a previous study, a 4:1 ratio of protein to glucose maximized the biocrude oil yield and a ratio of 3:1 maximized the biocrude oil productivity per gram protein compared to the control, which was attributed to the Maillard reaction. This result indicated that the Maillard reaction might have been enhanced at incubation temperatures greater than 35 °C due to the formulation of the ideal ratio of glucose to protein. 32

Finally, a third explanation could be the production of an increased content of fatty acids at higher DF incubation temperatures (Figure S3). The presence of an increased acid content could have lowered the pH and catalyzed degradation of carbohydrates. Previous studies noted that a low pH promoted the biocrude oil yield under reaction temperatures ranging from 275 to 320  $^{\circ}$ C. Thence, integrated DF-HTL was conducted using the DF-H conditions since it yielded the most H<sub>2</sub> among all trial runs (Figure 1).

3.3. Integrated Dark Fermentation and Hydrothermal Liquefaction (DF-HTL). 3.3.1. DF-HTL Comprehensive Evaluation. A Sankey diagram was constructed to elucidate the elemental and energy balance of the HTL and DF-HTL processes (Figure 4). Energy balance results demonstrated that the energy of the initial feedstock was almost equally distributed into the oil and aqueous phases, amounting to 48.5 and 50.3%, respectively. However, for DF-HTL, 66.1% of the energy was distributed into the oil and only 31.0% was distributed into the aqueous phase. A similar trend was exhibited for the carbon balance, in which the carbon distribution of oil in the control was initially 41.3% and increased to 52.5% for DF-HTL. Conversely, the carbon in the aqueous phase reduced from 43.5% for the control to 26.8% for DF-HTL. However, the nitrogen balance results were not favorable. Specifically, the nitrogen distribution from the control to DF-HTL in the biocrude oil increased from 26.4 to 39.1% and decreased in the aqueous phase from 70.3 to

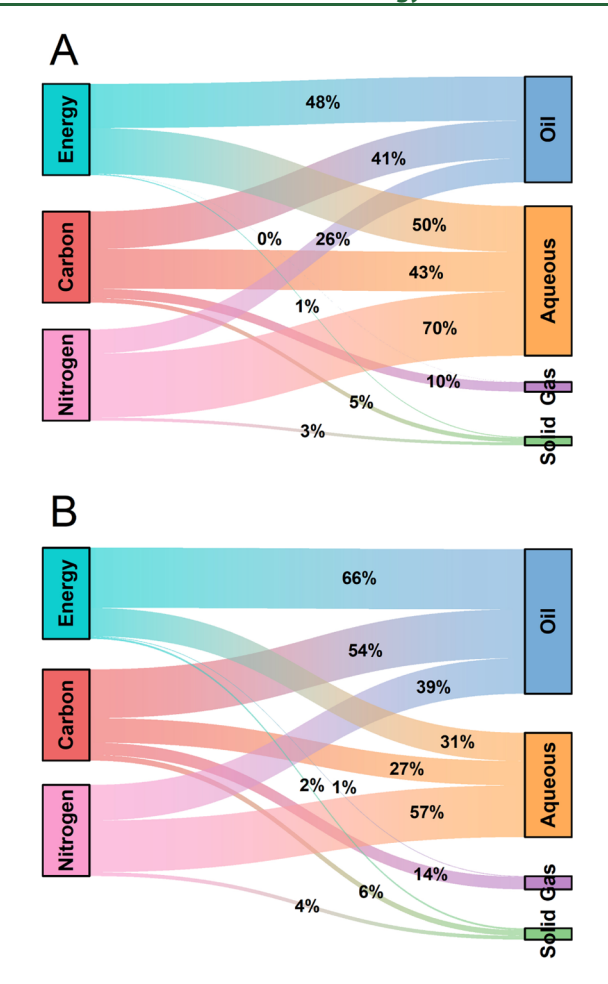


Figure 4. Investigation of the carbon, nitrogen, and energy balance of the control (A) and DF-HTL conversion processes (B). HTL of the control was conducted at a temperature of 340  $^{\circ}$ C and a retention time of 50 min. DF-HTL was conducted by first conducting DF at 55  $^{\circ}$ C and then subsequently conducting HTL at a temperature of 340  $^{\circ}$ C and a retention time of 50 min in the same reactor.

56.7%. This further emphasizes the need for biocrude oil upgrading. However, DF-HTL could be beneficial for subsequent valorization of the aqueous phase because reduced distribution of carbon and nitrogen is conducive to aqueous phase recycling, biological conversion, etc. <sup>34,35</sup> Since DF-HTL only dramatically influenced the biocrude oil and aqueous phase, these two reaction products were investigated in detail. Additional information concerning the solid residue and gaseous phase products is provided in the Supporting Information (Tables S5 and S6).

3.3.2. Impact on Biocrude Oil Characteristics. Notably, DF-HTL resulted in a significant 9.8% increase in the biocrude oil yield compared to the control. Mass balance and nutrient balances between the control and DF-HTL are provided in the Supporting Information (Figures S5, S6, and Table S7). With regard to the impact of DF-HTL on the biocrude oil yield, a previous study noted that the usage of hydrogen as a process gas led to a higher oil production efficiency (~45–75%) compared to using a headspace gas of N<sub>2</sub> (~30–65%). Another point to note is that for the DF-HTL conditions, the headspace gas was not purged as it was in the separated DF and HTL of algae experiments (DF-L, DF-M, and DF-H). Thus, the pressure of H<sub>2</sub> may have also improved the biocrude oil yield. A previous study demonstrated that sparging H<sub>2</sub>/CO<sub>2</sub>

at a ratio of 4:1 could enhance the production of carboxylic acids via acidogenic fermentation by 1.3-fold compared with the control (evacuation of the headspace).<sup>37</sup>

The production of carboxylic acids may have also enhanced the decomposition of the post-treatment material, leading to a greater production of biocrude oil. Zhu et al. previously discovered that the presence of acids enhanced the decomposition of barley straw, and these acids may have been involved in the formation of liquefied products. This was further corroborated by a preceding study that found that the addition of organic acids greatly enhanced the hydrothermal degradation of lignocellulosic biomass model compounds. Thus, the synergistic effect of DF-HTL is particularly prominent for carbohydrate-rich feedstocks.

With regard to the quality of the biocrude oil, Figure 5 demonstrates the quantitative impact of DF-HTL on the biocrude oil characteristics in comparison to the control. DF-HTL led to a 5.1% decrease in the accumulation of N- and Ocontaining heterocycles (Figure 5A). This could have been caused by the deamination process during DF in which the peptide bond of proteins would be cleaved, leaving the amino acids more susceptible to degradation and eventual release as ammonia in the aqueous phase. It was previously determined that the biodegradability of proteins was much faster (0.84 day<sup>-1</sup>) than carbohydrates (0.55 day<sup>-1</sup>). The relative content of fatty acid derivatives increased in the biocrude oil by 8.9%. This validated the hypothesis that DF-HTL processing could have produced an enhanced fatty acid content, which could augment the biocrude oil yield. Previous studies have shown that the acidogenic bacteria converted the reactants produced from hydrolysis to an array of compounds including H2 and fatty acids.40 Thus, DF-HTL could have led to the initial production of fatty acids through hydrolysis and subsequent conversion of carbohydrates and these compounds were distributed into the biocrude oil.

Elemental analysis of the biocrude oil demonstrated that DF-HTL led to a slight decrease in the carbon (1.0 wt %) and oxygen contents (0.6 wt %), a moderate increase in the hydrogen content (1.8 wt %), and a significant increase in the nitrogen content (8.5 wt %) compared with the control (Figure 5B and Table S8). Since the GC-MS data did not display an increase in N-containing moieties, it is hypothesized that these compounds may have been nonvolatile, medium-to high-molecular weight compounds (200–500 Da) with a vaporization point above the GC-MS column temperature (e.g., melanoidin derivatives derived from the Maillard reaction).

Figure 5C depicts the MALDI results for the DF-HTL biocrude oil. DF-HTL (relative abundance of 0.38) led to an aggregation of compounds within the 200-400 Da molecular weight range compared to the control (relative abundance of 0.31). This group of compounds could have been attributed to fatty acid derivatives (octadecanamide, hexadecanoic acid, dodecanamide), piperazinedione derivatives, etc. This also resulted in the biocrude oil derived from DF-HTL having a lower average molecular weight (559 Da) compared to the control (588 Da). The initial conversion of protein peptides and carbohydrate polymers to subsequent sugar and amino acid monomers may have led to an overall decrease in the molecular weight of the resulting oil compounds. This initial conversion may have decreased the molecular weight of the compounds by limiting the impact of repolymerization reactions. This can be specifically seen by observing that the

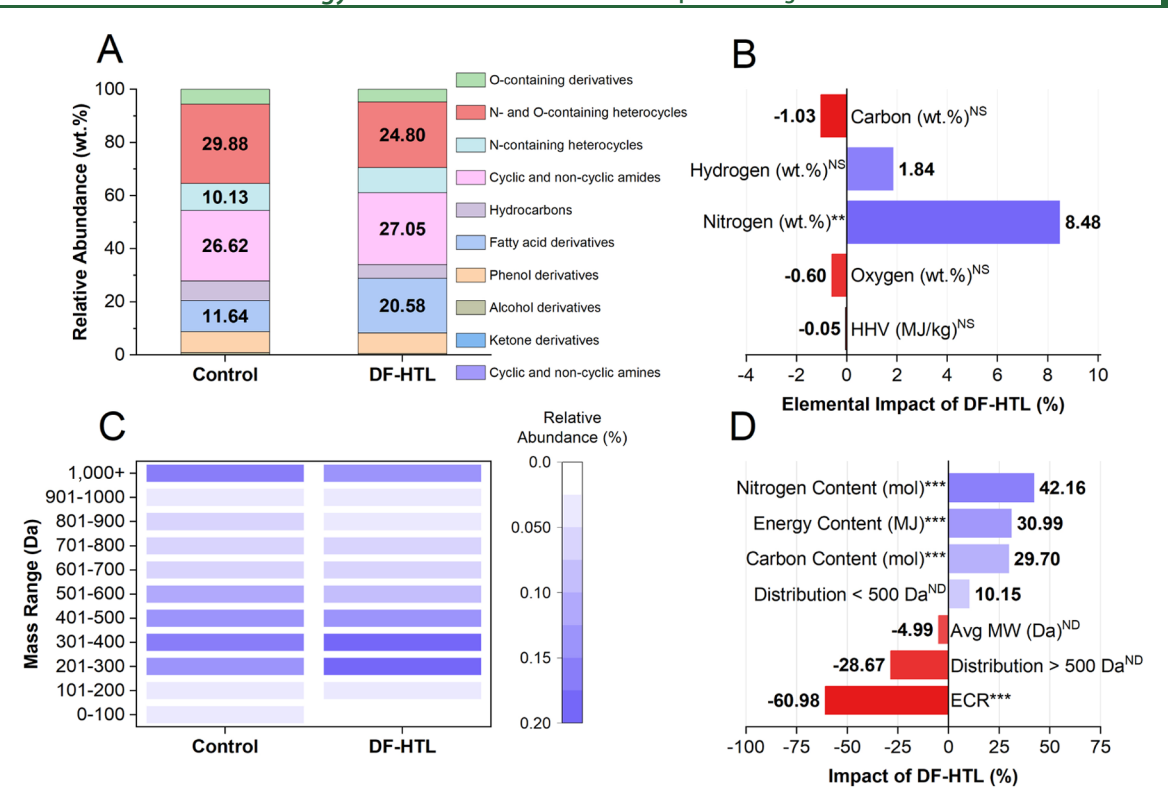


**Figure 5.** Influence of DF-HTL on the chemical makeup (A), the elemental makeup (B), and the molecular weight distribution (C) of the biocrude oil. The quantitative impact of DF-HTL on the biocrude oil (D). \*Denotes p-value <0.10, \*\*denotes p-value <0.05, \*\*\*denotes p-value <0.01, NS denotes a lack of statistical significance between the treatment and control (p > 0.1), and ND denotes that the significance was not detected due to a lack of duplicate samples.

distribution of compounds with a molecular weight above 1000 Da decreased by 8.4% compared to the control.

Figure 5D reports an evaluation taking into account both yields and elemental characteristics of the biocrude oil. Most notably, DF-HTL significantly increased the oil production (wt %) and carbon content (mol) of the biocrude oil by 9.8 and 29.7%, respectively. This in turn led to the biocrude oil harnessing a 31.0% greater energy content (MJ), and it led to a reduction in the energy conversion ratio (ECR) by 61.0%. ECR is defined as the ratio between the energy needed to produce biocrude oil (MI) and the energy released by combusting biocrude oil.41 An ECR value lower than one indicates a net energy gain of the system, and the higher the value of the ECR, the more energy needed for the conversion process. 10,41 However, DF-HTL acts as a double-edged sword: on the one hand, DF-HTL increased the carbon content, energy content, and overall quantity of biocrude oil. On the other hand, DF-HTL also increased the nitrogen content (mol) in the biocrude oil by 42.2%. Therefore, it is clear that DF-HTL involves an interaction between carbohydrates and proteins that augments the production of biocrude oil while simultaneously shifting the distribution of nitrogen to the biocrude oil.

3.3.3. Impact on Aqueous Phase Characteristics. DF-HTL resulted in a significant 19.0% decrease in the aqueous yield (wt %) compared to the control (Figure S6). Notably, the relative concentration (wt %) of N- and O-containing heterocycles decreased by 8.4% and the relative concentration of fatty acid derivatives increased by 8.7% (Figure 6A). This trend was identical to that of the biocrude oil. Thus, these two categories of compounds were the most susceptible to DF-HTL processing for both biocrude oil and aqueous products. It

is hypothesized that DF could break down the carbohydrate polymers into aqueous-soluble substrates. This could potentially enhance the interaction between proteins and carbohydrates, which could be attributed to the increase in the biocrude oil yield and the decrease of the aqueous yield. With regard to the elemental composition, Figure 6B illustrates that both the ammonia nitrogen and total nitrogen concentrations increased from 4.51 to 5.42 g/L and 7.72 to 9.75 g/L from the control to DF-HTL, respectively. This validates the hypothesis that DF may have led to an increase in the deamination of proteins to yield small molecular weight compounds or ammonia, which preferentially distributed into the aqueous phase. Moreover, DF-HTL decreased the COD of the aqueous phase by 31.8% (Table S9). However, it should be noted that despite the fact that the concentration of nitrogen increased in the aqueous phase, the aqueous phase yield was far less for DF-HTL (28.2%) compared to the control (47.2%) (Figure S6). Thus, accounting for the yield and concentration, the nitrogen content in the aqueous phase derived from DF-HTL decreased in comparison to the control (Figure 6F).

With regard to the MALDI results, DF-HTL increased the average molecular weight by 18.2% and decreased the distribution of compounds with a molecular weight <400 Da by 7.7% compared to the results from the control (Figure 6C,F). This data signified that DF-HTL led to the accumulation of heavier chemical compounds compared with the aqueous phase derived from the control.

To better understand the chemical characteristics of the aqueous phase of the control and DF-HTL, high-resolution LC-MS was conducted (Figure 6D,E). The compounds that exhibited the largest changes between the control and DF-HTL in the descending order were *trans*-2-aminomethyl-1-

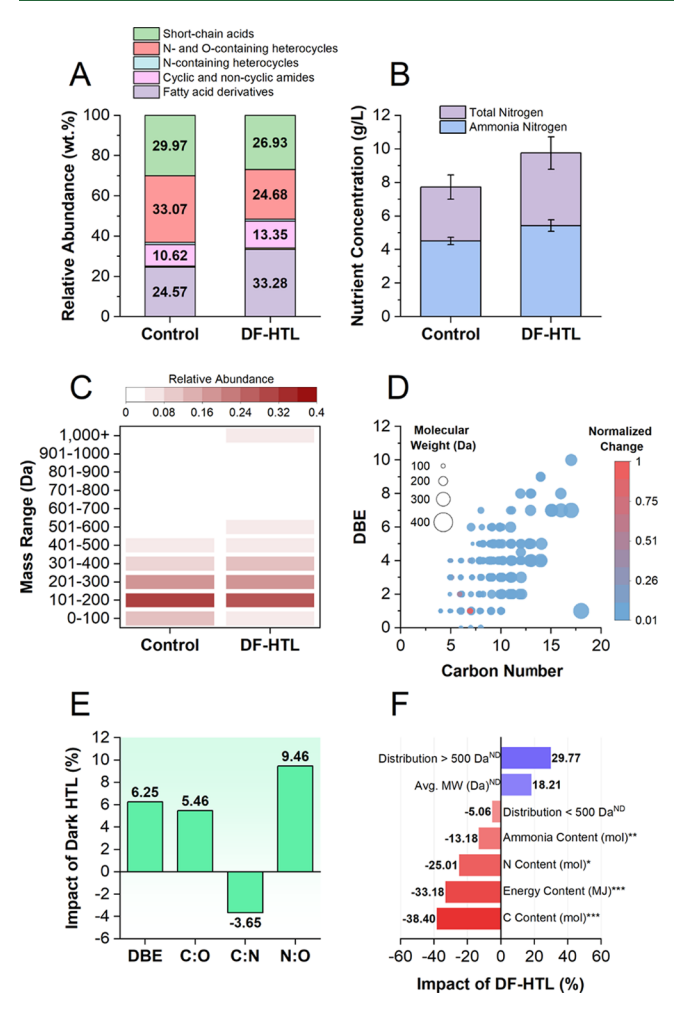


**Figure 6.** Impact of DF-HTL on the distribution of organic compounds (A), nutrients (B), and molecular weight distribution (C) of the aqueous phase. Normalized change in the concentration of organic compounds in the aqueous phase (D). Compounds most impacted by DF-HTL (E). Quantitative influence of DF-HTL on the characteristics of the aqueous phase (F). \*Denotes p-value <0.10, \*\*denotes p-value <0.05, \*\*\*denotes p-value <0.01, NS denotes a lack of statistical significance between the treatment and control (p > 0.1), and ND denotes that the significance was not detected due to a lack of duplicate samples.

cyclohexanol, 6-aminocaproic acid, caprolactam, and 3-hydroxypyridine. The presence of these compounds decreased in the DF-HTL run compared to that in the control with the exception of 3-hydroxypyridine. Thus, the compounds most impacted by DF-HTL were compounds with N- and O-containing functional groups. This further verifies the validity of the GC-MS results for the aqueous phase.

The double bond equivalents (DBE) increased by 6.3%. This inferred that DF-HTL led to an increased level of unsaturation (rings and double bonds) in the aqueous phase compared to the control. These results were in line with the MALDI results. Furthermore, the C/O, C/N, and N/O elemental number ratios exhibited changes of 5.5, -3.7, and 9.5%, respectively (Figure 6E). This implied that DF-HTL led to a greater interaction of nitrogen- and oxygen-containing compounds in the aqueous phase, thereby elucidating that the main compounds that were impacted via DF-HTL were N-and O-containing derivatives.

Figure 6F provides a depiction of the quantitative impact of DF-HTL on the aqueous phase incorporating both aqueous phase quality data (elemental composition, molecular weight, etc.) and gravimetric data. DF-HTL significantly reduced the production of aqueous-soluble compounds (wt %) by 19.0%, decreased the nitrogen content (mol) by 25.0%, lowered the carbon content (mol) by 38.4%, and decreased the energy content (MJ) by 33.2%. However, DF-HTL also led to an aqueous phase that was much heavier, amounting to an increase in the molecular weight (Da) by 18.2% and an increase in the distribution of compounds with a molecular weight greater than 500 Da of 29.8%.

**3.4. Dark HTL Reaction Pathway.** Model compound tests were conducted to represent the different states of DF-HTL. Cellulose, glucose, and acetic acid were combined with protein at a 1:1 ratio to mimic the following conditions: cessation of carbohydrate polymer cross-linkage networks (C-P), cleavage of carbohydrate polymer  $\beta$ -1,4-glycosidic linkages (G-P), and hydrolysis and subsequent glycolysis of glucose monomers (A-P). From the results presented in Figure S7, it is clear that pure protein was most beneficial for promoting the biocrude oil yield, with protein leading to a biocrude oil content of 29.5% and G-P leading to the lowest biocrude oil yield of 16.6% at a 1:1 protein to carbohydrate ratio. Additional data for the model compound experiments are provided in the Supporting Information (Figures S8, S9 and Tables S10, S11).

However, protein productivity is a more objective way of assessing the impact of protein on the reaction products, since all trials are normalized according to their protein content. Notably, all binary interactions enhanced the productivity of protein distributed into the biocrude oil. Interactions with cellulose (C-P) and acetic acid (A-P) enhanced the protein productivity for biocrude oil production the most by 17.1 and 12.2%, respectively (Figure S7B). It is clear that changes in the oil yield were at the expense of compounds shifting from the aqueous phase to the biocrude oil phase. Thus, it can be surmised that the Maillard reaction tended to shift the contribution of proteins from the aqueous phase to the oil and solid phases, depending upon the binary interaction, amounting to decreases in the aqueous protein contribution between 13.7 and 30.9%.

Based on the quantitative results from DF-HTL and model compound chemical analysis results, a reaction pathway diagram was proposed to explain the chemical pathway for the biocrude oil and aqueous phase chemical products (Figure 7). DF-HTL led to the production of an increased content of fatty acid derivatives via acidogenesis. These products could undergo decarboxylation to form aliphatics, amination to form fatty acid amides, or hydrogenation/dehydrogenation to form saturated/unsaturated fatty acids, which were then subjected to biocrude oil. In particular, DF-HTL increased the contents of hexadecanoic acid and hexadecanamide in the biocrude oil by 174.2 and 37.2% compared to the control, respectively. In addition, the increased acid content (acetic acid, propanoic acid, butanoic acid) could catalyze the hydrolysis of carbohydrates leading to the production of a greater amount of monosaccharide-derived products (glucose, fructose, galactose, etc.). These compounds subsequently underwent decomposition to form a variety of reaction products. Most notably, accelerated hydrolysis and decomposition would lead to an increased production of ketones/aldehydes and furfural intermediates. Ketones/aldehydes and furfurals are key components in the Maillard reaction, which could signify

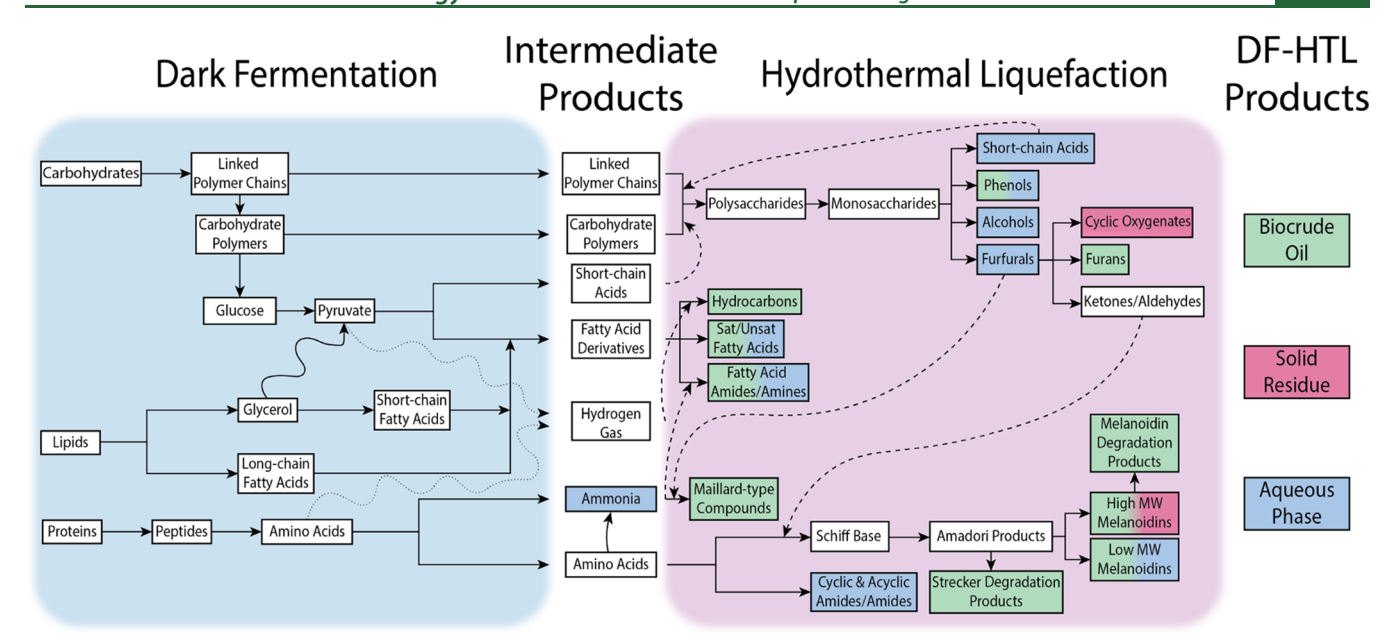


Figure 7. Proposed reaction pathway for DF-HTL processing. Dashed lines indicate that the component is used as a coproduct for a chemical reaction. Dotted lines signify the conversion of a product to hydrogen. White boxes represent the intermediates; the green, red, and blue boxes represent the organics remaining in the biocrude oil, solid residue, and aqueous phase, respectively.

that the increased presence of Maillard reaction reactants could accelerate the production of Maillard reaction degradation products, according to Le Chatlier's principle. Another study noted that at low reaction temperatures (<260 °C) melanoidin polymers could form due to the Maillard reaction, which caused an adverse effect on the biocrude oil yield. However, at elevated temperatures, these compounds could be decomposed into cyclic monomers (pyrazine, pyrroles, etc.). 42 For instance, DF-HTL increased the presence of 2-piperidinone by 156.4% compared to the control. Specifically, furfurals and ammonia can react to form Maillard-type compounds (2-methyl-5hydroxypyridine, 5-methyl-2-formylpyrrole, etc.), which have been detected in the biocrude oil. 43 Examples of these types of compounds in the DF-HTL oil include acetylpyrrolidine, 2ethyl-6-methyl-pyrazine, and 6-methyl-3-pyridinol, which all increased in comparison to the control by 51.7, 45.4, and 67.1%, respectively. Similar Maillard-type compounds can also be generated via condensation reactions involving ammonia and aldehydes, ketones, or unsaturated carbonylic compounds.43,

In addition, other N- and O-containing derivatives can be derived from the reaction of amino acids with ketones/ aldehydes. First, amino acids can react with ketones/aldehydes to form a Schiff base (resulting in the formation of a C=N bond), form diketopiperazines through the condensation of amino acids, or form N-containing derivatives from the cleavage of amino acid side chains. Subsequently, the Schiff base undergoes an Amadori rearrangement, involving an intramolecular redox reaction that converts the Schiff base (imine derivative) into a ketoamine.<sup>45</sup> The Amadori products can then undergo degradation through decarboxylation and deamination or oxidation to form Strecker degradation products (aldehydes, keto acids, etc.). Amadori product degradation also yields highly reactive dicarbonyls, which act as propagators and continually react with free amino groups, thereby leading to the formation of cross-linking melanoidin products. 46 However, the definitive structure of melanoidins is not clear due to the chemical complexity of these compounds.

Previous researchers have described melanoidin derivatives as being repeating units of furans and pyrroles, while others have described them as polymers constituted by sugar degradation products and branched amino compounds. 47,48

It should be noted that GC-MS and elemental analysis techniques only provide an indirect method of elucidating the reaction pathway for the DF-HTL process. Other techniques need to be explored to better understand the influence of the DF-HTL process on the quality of the reaction products. Fourier-transform ion cyclotron resonance (FT-ICR) mass spectrometry is one such technique that holds promise because it can apply a petroleomic approach to accurately assess the oil chemical makeup. For example, FT-ICR can be used to formulate isoabundance contour plots to better understand the formation and degradation of Maillard reaction products during the DF-HTL process through analysis of the heteroatom class (O2, N1O3, N2O3, etc.) and DBE.49 In addition, online product monitoring techniques (TG-MS, TG-FTIR, etc.) should be incorporated to understand the timeand temperature-dependent dynamic production of oil reaction products derived from carbohydrate-protein interactions to better understand the DF-HTL process.<sup>5</sup>

# 4. PROSPECTS AND TECHNOLOGICAL APPLICATIONS

DF-HTL is advantageous for enhancing the carbon and energy recovery of biocrude oil, which could be further upgraded to yield value-added transportation fuels and chemicals. One matter of concern is the increased nitrogen content in the biocrude oil, which may increase the economic input associated with hydrogenation, hydrodenitrogenation, adsorption, and liquid—liquid extraction upgrading processes. Further, oil with a high nitrogen content can lead to gum formation, catalyst inhibition, corrosion, and metal complexation. However, biocrude oil with a high nitrogen content could be used as a lubricating oil, since engine oil dispersants and detergents containing nitrogen are frequently used to prevent sludge formation in the engine and control

oxidation. <sup>52</sup> Furthermore, a previous study noted that most nitrogen-containing compounds are concentrated in the heavier distillate range. <sup>53</sup> Thus, oil derived from DF-HTL processing would be more suitable for fuels associated with a low distillate temperature range, such as naphtha, gasoline, and kerosene. Further, high-value nitrogenous compounds that are frequently used in polymer, pharmaceutical, and even anticancer medicinal industries (e.g., pyridine, quinolone, indole, etc.) can be extracted from the biocrude oil. <sup>54</sup> Thus, although a high nitrogen content is disadvantageous in some aspects, it is advantageous in other aspects.

As for the aqueous product, due to the reduced carbon and energy subjected to the aqueous phase, the DF-HTL aqueous phase would be easier to treat, leading to lower economic costs for aqueous phase treatment and disposal. This is a critical improvement, because to achieve the Department of Energy's performance goal (\$3.18–3.33/GGE) by 2022, serious cost reductions need to be made for HTL technology. Since aqueous phase treatment and biocrude production account for 17.9–18.3 and 15.4–18.3% of the fuel selling price, respectively, DF-HTL technology demonstrates promise as a means to reduce the economic burden on these two reaction products, since this method addresses both products concomitantly.<sup>55</sup>

The promising results from DF-HTL could lead to benefits outside of the production quantity and quality of biocrude oil. For example, the DF-HTL process could enhance the fluidity of the biocrude oil product. Previous studies have indicated that pumpability of the substrate is a limiting factor for the continuous production of biocrude oil. Soluble compounds, such as fatty acids, amino acids, and monosaccharides, are produced via hydrolysis and acidogenesis of solid particles within the feedstock, which leads to an increase of the fluidity of the substrate. Thus, the DF-HTL process could be an alternative to mechanical, technical, or chemical treatment techniques to ensure a homogeneous, pumpable slurry while aiding in the enhancement of the oil yield for continuous processes.

The DF-HTL process is conducive to feedstocks with a high carbohydrate, high protein, and low lipid content, which traditionally yield a poor biocrude oil yield. Specifically, the DF-HTL process holds promise as a method to treat agricultural residues and food waste to enhance their potential for producing a large quantity of biocrude oil. Despite its advantageous aspects, the DF-HTL process still needs to be analyzed from an economic and emissions perspective. Techno-economic analysis and life cycle assessments need to be obtained to determine the environmental implications of combining these two conversion technologies.

#### ASSOCIATED CONTENT

#### Supporting Information

The Supporting Information is available free of charge at https://pubs.acs.org/doi/10.1021/acs.est.0c05924.

Pictures of Lake Tainter, WI algal bloom microalgae retrieval site (left), and the algae collection and filtration process using a mesh sieve (right) (Figure S1); GC-MS results for the biocrude oil derived from the control and the HTL of fermented algae (DF-L, DF-M, and DF-H) conducted at a temperature of 340 °C and a retention time of 50 min (Figure S2); GC-MS results for the aqueous phase derived from the control and the HTL of

fermented algae (DF-L, DF-M, and DF-H) conducted at a temperature of 340 °C and a retention time of 50 min (Figure S3); mass distribution for the biocrude oil (A) and aqueous phase (B) derived from the HTL of fermented algae (DF-L, DF-M, and DF-H), average molecular weight of the biocrude oil (C), and the aqueous phase (D) (Figure S4); carbon (A) and nitrogen (B) balance for the control, separated DF and HTL of algae (DF-L, DF-M, DF-H), and integrated DF-HTL experiments (Figure S5); product balance comparison between DF-HTL and the control conducted at a temperature of 340 °C and a retention time of 50 min (Figure S6); model compound yields for protein and binary mixtures of cellulose-protein (C-P), glucose-protein (G-P), and acetic acid-protein (A-P) (A) (Figure S7); GC-MS results for the biocrude oil and aqueous phase of the primary and binary model carbohydrate and protein derivatives conducted at a temperature of 340 °C and a retention time of 50 min (Figure S8); mass distribution for the HTL of model primary and binary mixtures for the oil (A) and aqueous phase (B) (Figure S9); algal bloom microalgae proximate and ultimate analysis (Table S1); algal bloom microalgae metal analysis (Table S2); water quality data from Lake Tainter, WI (Table S3); reaction setup for HTL (control), the HTL of fermented algae (DF-L, DF-M, and DF-H), DF-HTL, and model compound experiments (Table S4); elemental analysis of the solid residue derived from the control, HTL of fermented algae (DF-L, DF-M, and DF-H), and DF-HTL (Table S5); composition of the HTL gaseous phase (Table S6); analysis of variance (ANOVA) results comparing the control, HTL of fermented algae (DF-L, DF-M, and DF-H), and DF-HTL trial product yields (Table S7); elemental analysis of the biocrude oil derived from the control, HTL of fermented algae (DF-L, DF-M, and DF-H), and DF-HTL (Table S8); chemical oxygen demand (COD) of the aqueous phase derived from the control and DF-HTL experiments (Table S9); elemental analysis of the oil produced from the HTL of primary and binary mixtures of carbohydrate and protein model compounds (Table S10); elemental analysis of the solid residue produced from the HTL of primary and binary mixtures of carbohydrate and protein model compounds (Table S11); and two paragraphs about the methodology used to conduct feedstock metal analysis and wastewater quality analysis (p S21) (PDF)

#### AUTHOR INFORMATION

#### **Corresponding Authors**

Yuanhui Zhang — Department of Agricultural & Biological Engineering, University of Illinois at Urbana—Champaign, Urbana, Illinois 61801, United States; oocid.org/0000-0003-1387-5618; Email: yzhang1@illinois.edu

Buchun Si — Laboratory of Environment-Enhancing Energy (E2E), Key Laboratory of Agricultural Engineering in Structure and Environment, Ministry of Agriculture, College of Water Resources and Civil Engineering, China Agricultural University, Beijing 100083, P. R. China; Email: sibuchun@cau.edu.cn

#### **Authors**

- Jamison Watson Department of Agricultural & Biological Engineering, University of Illinois at Urbana—Champaign, Urbana, Illinois 61801, United States
- Megan Swoboda Department of Agricultural & Biological Engineering, University of Illinois at Urbana—Champaign, Urbana, Illinois 61801, United States
- Aersi Aierzhati Department of Agricultural & Biological Engineering, University of Illinois at Urbana-Champaign, Urbana, Illinois 61801, United States
- Tengfei Wang College of Environmental Science and Engineering, Hunan University, Changsha 410082, P. R. China

Complete contact information is available at: https://pubs.acs.org/10.1021/acs.est.0c05924

#### **Notes**

The authors declare no competing financial interest. All authors have read and have abided by the statement of ethical standards.

#### ■ ACKNOWLEDGMENTS

The authors acknowledge the financial support provided by the National Science Foundation U.S.—China INFEWS grant (NSF# 18-04453 and 1744775), the National Natural Science Foundation of China (NSFC 51806243), and the Jonathan Baldwin Turner Ph.D. Fellowship provided by the University of Illinois at Urbana—Champaign.

### **■** REFERENCES

- (1) Woodward, G.; Gessner, M. O.; Giller, P. S.; Gulis, V.; Hladyz, S.; Lecerf, A.; Malmqvist, B.; McKie, B. G.; Tiegs, S. D.; Cariss, H.; Dobson, M.; Elosegi, A.; Ferreira, V.; Graca, M. A. S.; Fleituch, T.; Lacoursiere, J. O.; Nistorescu, M.; Pozo, J.; Risnoveanu, G.; Schindler, M.; Vadineanu, A.; Vought, L. B. M.; Chauvet, E. Continental-Scale Effects of Nutrient Pollution on Stream Ecosystem Functioning. *Science* 2012, 336, 1438–1440.
- (2) EPA, U.S.E.P.A. *The Facts about Nutrient Pollution*; United States Environmental Protection Agency, 2012; pp 1–2.
- (3) Nie, J.; Feng, H.; Witherell, B. B.; Alebus, M.; Mahajan, M. D.; Zhang, W.; Yu, L. Causes, Assessment, and Treatment of Nutrient (N and P) Pollution in Rivers, Estuaries, and Coastal Waters. *Curr. Pollut. Rep.* 2018, 4, 154–161.
- (4) Wolf, D.; Georgic, W.; Klaiber, H. A. Reeling in the damages: Harmful algal blooms' impact on Lake Erie's recreational fishing industry. *J. Environ. Manage.* **2017**, *199*, 148–157.
- (5) Sakamoto, S.; Lim, W. A.; Lu, D.; Dai, X.; Orlova, T.; Iwataki, M. Harmful algal blooms and associated fisheries damage in East Asia: Current status and trends in China, Japan, Korea and Russia. *Harmful Algae* 2020, No. 101787.
- (6) Farley, M. Eutrophication in Fresh Waters: An International Review. In *Encyclopedia of Lakes and Reservoirs*; Bengtsson, L.; Herschy, R. W.; Fairbridge, R. W., Eds.; Springer: Netherlands, 2012; pp 258–270.
- (7) Chen, W. T.; Qian, W.; Zhang, Y.; Mazur, Z.; Kuo, C. T.; Scheppe, K.; Schideman, L. C.; Sharma, B. K. Effect of ash on hydrothermal liquefaction of high-ash content algal biomass. *Algal Res.* **2017**, *25*, 297–306.
- (8) DOE (U.S. Department of Energy). National Algal Biofuels Technology Review; Office of Energy Efficiency & Renewable Energy, Bioenergy Technologies Office, 2016.
- (9) Tian, C.; Li, B.; Liu, Z.; Zhang, Y.; Lu, H. Hydrothermal liquefaction for algal biorefinery: A critical review. *Renewable Sustainable Energy Rev.* **2014**, *38*, 933–950.

- (10) Chen, W.-T. Upgrading Hydrothermal Liquefaction Biocrude Oil from Wet Biowaste into Transportation Fuel. University of Illinois at Urbana—Champaign, 2017.
- (11) Leow, S.; Witter, J. R.; Vardon, D. R.; Sharma, B. K.; Guest, J. S.; Strathmann, T. J. Prediction of microalgae hydrothermal liquefaction products from feedstock biochemical composition. *Green Chem.* **2015**, *17*, 3584–3599.
- (12) Tian, C.; Liu, Z.; Zhang, Y.; Li, B.; Cao, W.; Lu, H.; Duan, N.; Zhang, L.; Zhang, T. Hydrothermal liquefaction of harvested high-ash low-lipid algal biomass from Dianchi Lake: Effects of operational parameters and relations of products. *Bioresour. Technol.* **2015**, *184*, 336–343.
- (13) Zhu, Z.; Si, B.; Lu, J.; Watson, J.; Zhang, Y.; Liu, Z. Elemental migration and characterization of products during hydrothermal liquefaction of cornstalk. *Bioresour. Technol.* **2017**, *243*, 9–16.
- (14) Li, H.; Liu, Z.; Zhang, Y.; Li, B.; Lu, H.; Duan, N.; Liu, M.; Zhu, Z.; Si, B. Conversion efficiency and oil quality of low-lipid high-protein and high-lipid low-protein microalgae via hydrothermal liquefaction. *Bioresour. Technol.* **2014**, *154*, 322–329.
- (15) Li, Q.; Hu, X.; Liu, D.; Song, L.; Yan, Z.; Li, M.; Liu, Q. Comprehensive evaluation of hydro-liquefaction characteristics of lignocellulosic subcomponents. *J. Energy Inst.* **2020**, 93, 1705–1712.
- (16) Ding, C.; Yang, K.-L.; He, J. Biological and fermentative production of hydrogen. In *Handbook of Biofuels Production*, 2nd ed.; Luque, R.; Lin, C. S. K.; Wilson, K.; Clark, J., Eds.; Woodhead Publishing, 2016; pp 303–333.
- (17) Xia, A.; Cheng, J.; Murphy, J. D. Innovation in biological production and upgrading of methane and hydrogen for use as gaseous transport biofuel. *Biotechnol. Adv.* **2016**, *34*, 451–472.
- (18) Łukajtis, R.; Hołowacz, I.; Kucharska, K.; Glinka, M.; Rybarczyk, P.; Przyjazny, A.; Kamiński, M. Hydrogen production from biomass using dark fermentation. *Renewable Sustainable Energy Rev.* 2018, 91, 665–694.
- (19) Peralta-Yahya, P. P.; Zhang, F.; Del Cardayre, S. B.; Keasling, J. D. Microbial engineering for the production of advanced biofuels. *Nature* **2012**, *488*, 320–328.
- (20) Long, J. H.; Aziz, T. N.; Reyes, F. L. D. L.; Ducoste, J. J. Anaerobic co-digestion of fat, oil, and grease (FOG): A review of gas production and process limitations. *Process Saf. Environ. Prot.* **2012**, 90, 231–245.
- (21) Harris, P. W.; McCabe, B. K. Review of pre-treatments used in anaerobic digestion and their potential application in high-fat cattle slaughterhouse wastewater. *Appl. Energy* **2015**, *155*, 560–575.
- (22) Oh, S. E.; Van Ginkel, S.; Logan, B. E. The Relative Effectiveness of pH Control and Heat Treatment for Enhancing Biohydrogen Gas Production. *Environ. Sci. Technol.* **2003**, *37*, 5186–5190.
- (23) Aierzhati, A.; Stablein, M. J.; Wu, N. E.; Kuo, C. T.; Si, B.; Kang, X.; Zhang, Y. Experimental and model enhancement of food waste hydrothermal liquefaction with combined effects of biochemical composition and reaction conditions. *Bioresour. Technol.* **2019**, 284, 139–147.
- (24) Qiu, Y.; Aierzhati, A.; Cheng, J.; Guo, H.; Yang, W.; Zhang, Y. Biocrude Oil Production through the Maillard Reaction between Leucine and Glucose during Hydrothermal Liquefaction. *Energy Fuels* **2019**, *33*, 8758–8765.
- (25) Lu, J.; Zhang, J.; Zhu, Z.; Zhang, Y.; Zhao, Y.; Li, R.; Watson, J.; Li, B.; Liu, Z. Simultaneous production of biocrude oil and recovery of nutrients and metals from human feces via hydrothermal liquefaction. *Energy Convers. Manage.* **2017**, *134*, 340–346.
- (26) Chen, W. T.; Zhang, Y.; Zhang, J.; Yu, G.; Schideman, L. C.; Zhang, P.; Minarick, M. Hydrothermal liquefaction of mixed-culture algal biomass from wastewater treatment system into bio-crude oil. *Bioresour. Technol.* **2014**, *152*, 130–139.
- (27) Adarme, O. F. H.; Baêta, B. E. L.; Lima, D. R. S.; Gurgel, L. V. A.; de Aquino, S. F. Methane and hydrogen production from anaerobic digestion of soluble fraction obtained by sugarcane bagasse ozonation. *Ind. Crops Prod.* **2017**, *109*, 288–299.

- (28) Milledge, J. J.; Nielsen, B. V.; Maneein, S.; Harvey, P. J. A brief review of anaerobic digestion of algae for BioEnergy. *Energies* **2019**, *12*. No. 1166.
- (29) Bobleter, O. Hydrothermal degradation of polymers derived from plants. *Prog. Polym. Sci.* **1994**, *19*, 797–841.
- (30) Domozych, D. S.; Ciancia, M.; Fangel, J. U.; Mikkelsen, M. D.; Ulvskov, P.; Willats, W. G. T. The cell walls of green algae: A journey through evolution and diversity. *Front. Plant Sci.* **2012**, *3*, No. 82.
- (31) Zhang, C.; Tang, X.; Sheng, L.; Yang, X. Enhancing the performance of Co-hydrothermal liquefaction for mixed algae strains by the Maillard reaction. *Green Chem.* **2016**, *18*, 2542–2553.
- (32) Srokol, Z.; Bouche, A. G.; Van Estrik, A.; Strik, R. C. J.; Maschmeyer, T.; Peters, J. A. Hydrothermal upgrading of biomass to biofuel; studies on some monosaccharide model compounds. *Carbohydr. Res.* **2004**, 339, 1717–1726.
- (33) Yin, S.; Tan, Z. Hydrothermal liquefaction of cellulose to biooil under acidic, neutral and alkaline conditions. *Appl. Energy* **2012**, 92, 234–239.
- (34) Biller, P.; Madsen, R. B.; Klemmer, M.; Becker, J.; Iversen, B. B.; Glasius, M. Effect of hydrothermal liquefaction aqueous phase recycling on bio-crude yields and composition. *Bioresour. Technol.* **2016**, 220, 190–199.
- (35) Andreozzi, R.; Insola, A.; Caprio, V.; D'Amore, M. G. Ozonation of pyridine in aqueous solution: Mechanistic and kinetic aspects. *Water Res.* **1991**, *25*, 655–659.
- (36) He, B. Thermochemical Conversion of Swine Manure to Produce Oil and Reduce Waste. Ph.D. Dissertation, University of Illinois at Urbana—Champaign, 2000.
- (37) Zhou, M.; Zhou, J.; Tan, M.; Du, J.; Yan, B.; Wong, J. W. C.; Zhang, Y. Enhanced carboxylic acids production by decreasing hydrogen partial pressure during acidogenic fermentation of glucose. *Bioresour. Technol.* **2017**, 245, 44–51.
- (38) Zhu, Z.; Rosendahl, L.; Toor, S. S.; Yu, D.; Chen, G. Hydrothermal liquefaction of barley straw to bio-crude oil: Effects of reaction temperature and aqueous phase recirculation. *Appl. Energy* **2015**, *137*, 183–192.
- (39) Li, Y.; Lu, X.; Yuan, L.; Liu, X. Fructose decomposition kinetics in organic acids-enriched high temperature liquid water. *Biomass Bioenergy* **2009**, 33, 1182–1187.
- (40) Khan, M. A.; Ngo, H. H.; Guo, W. S.; Liu, Y.; Nghiem, L. D.; Hai, F. I.; Deng, L. J.; Wang, J.; Wu, Y. Optimization of process parameters for production of volatile fatty acid, biohydrogen and methane from anaerobic digestion. *Bioresour. Technol.* **2016**, 219, 738–748.
- (41) Watson, J.; Lu, J.; de Souza, R.; Si, B.; Zhang, Y.; Liu, Z. Effects of the extraction solvents in hydrothermal liquefaction processes: Biocrude oil quality and energy conversion efficiency. *Energy* **2019**, *167*, 189–197.
- (42) Yang, W.; Li, X.; Li, Z.; Tong, C.; Feng, L. Understanding low-lipid algae hydrothermal liquefaction characteristics and pathways through hydrothermal liquefaction of algal major components: Crude polysaccharides, crude proteins and their binary mixtures. *Bioresour. Technol.* **2015**, *196*, 99–108.
- (43) Croce, A.; Battistel, E.; Chiaberge, S.; Spera, S.; De Angelis, F.; Reale, S. A Model Study to Unravel the Complexity of Bio-Oil from Organic Wastes. *ChemSusChem* **2017**, *10*, 171–181.
- (44) Hwang, H. I.; Hartman, T. G.; Ho, C. T. Relative Reactivities of Amino Acids in the Formation of Pyridines, Pyrroles, and Oxazoles. *J. Agric. Food Chem.* **1995**, 43, 2917–2921.
- (45) Yaylayan, V. A. Food Science and Technology Research Vol. 9, No. 1(2003). Nippon Shokuhin Kagaku Kogaku Kaishi 2003, 50, 372–377
- (46) Smaniotto, A.; Bertazzo, A.; Comai, S.; Traldi, P. The role of peptides and proteins in melanoidinb formation. *J. Mass Spectrom.* **2009**, *44*, 410–418.
- (47) Tressl, R.; Wondrak, G. T.; Garbe, L. A.; Krüger, R. P.; Rewicki, D. Pentoses and Hexoses as Sources of New Melanoidin-like Maillard Polymers. J. Agric. Food Chem. 1998, 46, 1765–1776.

- (48) Yaylayan, V. A.; Kaminsky, E. Isolation and structural analysis of Maillard polymers: Caramel and melanoidin formation in glycine/glucose model system. *Food Chem.* **1998**, *63*, 25–31.
- (49) Jarvis, J. M.; Billing, J. M.; Corilo, Y. E.; Schmidt, A. J.; Hallen, R. T.; Schaub, T. M. FT-ICR MS analysis of blended pine-microalgae feedstock HTL biocrudes. *Fuel* **2018**, *216*, 341–348.
- (50) Kumagai, S.; Yamasaki, R.; Kameda, T.; Saito, Y.; Watanabe, A.; Watanabe, C.; Teramae, N.; Yoshioka, T. Tandem μ-reactor-GC/MS for online monitoring of aromatic hydrocarbon production: Via CaOcatalysed PET pyrolysis. *React. Chem. Eng.* **2017**, *2*, 776–784.
- (51) Prado, G. H. C.; Rao, Y.; De Klerk, A. Nitrogen removal from oil: A review. *Energy Fuels* **2017**, *31*, 14–36.
- (52) Baker, M. Acylated Nitrogen Compounds Useful as Additives for Lubricating Oil and Fuel Compositions. US5,779,742A, 1998.
- (53) Audeh, C. A. Removal of Nitrogen Compounds from Lubricating Oils. *Ind. Eng. Chem. Prod. Res. Dev.* **1983**, 22, 276–279.
- (54) Yu, J.; Maliutina, K.; Tahmasebi, A. A review on the production of nitrogen-containing compounds from microalgal biomass via pyrolysis. *Bioresour. Technol.* **2018**, *270*, 689–701.
- (55) BTO. Multi-Year Program Plan Multi-Year Program Plan; Department of Energy's Building Technologies Office, 2016.
- (56) Watson, J.; Wang, T.; Si, B.; Chen, W. T.; Aierzhati, A.; Zhang, Y. Valorization of hydrothermal liquefaction aqueous phase: pathways towards commercial viability. *Prog. Energy Combust. Sci.* **2020**, *77*, No. 100819.